STUDIES OF REACTION KINETICS OF METHANE HYDRATE DISSOCIATION IN POROUS MEDIA

George J. Moridis*, Yongkoo Seol, and Timothy J. Kneafsey
Lawrence Berkeley National Laboratory
Earth Sciences Division
USA

ABSTRACT

The objective of this study is the description of the kinetic dissociation of CH_4-hydrates in porous media, and the determination of the corresponding kinetic parameters. Knowledge of the kinetic dissociation behavior of hydrates can play a critical role in the evaluation of gas production potential of gas hydrate accumulations in geologic media. We analyzed data from a sequence of tests of CH_4-hydrate dissociation by means of thermal stimulation. These tests had been conducted on sand cores partially saturated with water, hydrate and CH_4 gas, and contained in an x-ray-transparent aluminum pressure vessel. The pressure, volume of released gas, and temperature (at several locations within the cores) were measured. To avoid misinterpreting local changes as global processes, x-ray computed tomography scans provided accurate images of the location and movement of the reaction interface during the course of the experiments. Analysis of the data by means of inverse modeling (history matching) provided estimates of the thermal properties and of the kinetic parameters of the hydration reaction in porous media. Comparison of the results from the hydrate-bearing porous media cores to those from pure CH_4-hydrate samples provided a measure of the effect of the porous medium on the kinetic reaction. A tentative model of composite thermal conductivity of hydrate-bearing media was also developed.
Keywords: hydrate dissociation, porous medium, thermal stimulation, depressurization, kinetic parameters, thermal conductivity

NOMENCLATURE

A	Reaction area of dissociation [m^2]
C_H	Specific heat of the CH_4-hydrate [J/kg/K]
K_0	Intrinsic rate constant of the CH_4-hydrate dissociation reaction [$kg/m^2/Pa/s$]
k_H	Hydrate thermal conductivity [W/m/K]
k_W	Water thermal conductivity [W/m/K]
k_{Sd}	Thermal conductivity of dry sand [W/m/K]
k_{Sw}	Thermal conductivity of water-saturated sand [W/m/K]
k_Θ	Composite thermal conductivity [W/m/K]
N_H	Hydration number
m_H	Hydrate mass [kg]
f	Fugacity [Pa]
F_a	Interface area reduction factor
P	Pressure [Pa]
R	Gas constant [=8.314 J/mole/K]
S_G	Gas saturation
S_H	Hydrate saturation
S_W	Liquid water saturation
T	Temperature [K or ^oC]
ΔE	Activation energy of the CH_4-hydrate dissociation reaction [J/mol]
ϕ	Porosity

* Corresponding author: Phone: (510) 486-4746,
Fax: (510) 486-5686, E-mail: GJMoridis@lbl.gov

INTRODUCTION

Background

Vast amounts of hydrocarbons are trapped in hydrate deposits [1]. Current estimates of the worldwide quantity of hydrocarbon gas hydrates vary widely, and a range between 10^{15} to 10^{18} m^3 has been reported [1]. Note that these estimates are not the result of a systematic attempt to evaluate hydrate reserves, but are based on data obtained largely while investigating conventional hydrocarbon resources. Even by the most conservative estimates, the total quantity of gas in hydrates may surpass, by a factor of two, the energy content of the total fuel fossil reserves recoverable by conventional methods. The sheer magnitude of gas hydrate accumulations commands attention because of their potential as a substantial future energy resource.

Because of the strongly endothermic nature of the dissociation reaction and the importance of heat transfer, knowledge of the reaction kinetics and of the thermal properties of hydrate-bearing geological media is of critical importance to reliably pre-

dicting the gas production potential of natural gas hydrate deposits. The linear model of Bejan [2] is routinely used to describe the composite thermal conductivity k_Θ of multiphase systems in porous media [3], but it is not known if it is applicable to gas hydrates. The kinetic model of Kim et al. [4], as amended by Clarke and Bishnoi [5], is the only currently available model of the CH_4 hydration reaction: $CH_4 \cdot N_H H_2O = CH_4 + N_H H_2O(liq)$

However, this model was developed for pure hydrates undergoing dissociation under constant temperature conditions, and its applicability to hydrate dissociation in porous media is not known. Because of the effect of the pore structure and the geometry of the solid grain matrix on the size and surface area of the contiguous hydrate grains, as well as the potential impact of the grain surfaces and their physical/chemical properties on nucleation, such an environment appears to be substantially different from that of pure hydrates. This effort attempts to determine whether this difference translates into a difference in the reaction kinetics.

Objectives

The main objective of this study is to determine the parameters of the kinetic reaction of hydrate dissociation in porous media, based on the laboratory data discussed in the companion paper of Kneafsey et al. [6]. To the authors' knowledge, no previously published information on the subject exists. An additional objective, and a necessary step in the reaction kinetics study, is the estimation of the thermal properties of hydrate-bearing media and the development of quantitative relationships.

SYSTEM AND MODEL DESCRIPTION

The laboratory studies

The laboratory studies upon which our analysis is based were presented in detail in the companion paper of Kneafsey et al. [6], and will not be discussed further here. Additional information, elaborations and clarifications will be offered as the need arises in the course of this paper.

The numerical model

The numerical studies of hydrate system response were conducted using the TOUGH-Fx/HYDRATE simulator [7,8], which can model the non-isothermal hydration reaction, phase behavior, and flow of fluids and heat in complex geological media at any scale (from laboratory to reservoir) at which Darcy's law is valid. It includes both an equilibrium and a kinetic model [4,5] of hydrate formation and dissociation. The simulator accounts for heat and up to four mass components (i.e., water, CH_4, hydrate, and water-soluble inhibitors such as salts or alcohols) partitioned among four possible phases: gas, aqueous, ice and hydrate. The model can describe any combination of the possible hydrate dissociation mechanisms, i.e., depressurization, thermal stimulation, and inhibitor effects. By minimizing differences between observations and predictions (history-matching), the parameters of interest were determined using the method of Thomas and Hellums [9].

The thermal properties of the hydrate-bearing core were determined based on portions of the P and T datasets that corresponded to either hydrate stability or absence of hydrates in the pores. The iTOUGH2 inversion model [10] was used for these simulations. The fact that iTOUGH2 does not have hydrate capabilities is not an impediment because these studies involved determination of the composite thermal properties in a non-flowing and thermodynamically stable system.

Simulation Strategy and Approach

The simulation strategy aimed to limit uncertainty and the possibility of non-uniqueness in the solutions of the inverse problem. Thus, instead of attempting to determine the thermal properties and the kinetic parameters of dissociation simultaneously, the simulation effort was divided into two phases. The first phase focused on determining the thermal properties, and was based on P and T data before the formation of the hydrates or corresponding to stable hydrates.

By using these portions of the data sets, it was possible to concentrate on the thermal properties in relatively simple and stable thermodynamic states uncomplicated by the dissociation reaction. With the thermal properties considered known from the first phase, the second phase of the simulation focused entirely on the estimation of the kinetic parameters of the reaction based on the data set portion corresponding to the CH_4-hydrate dissociation.

THERMAL PROPERTY DETERMINATION

The simulation specifics

The simulated system is depicted in Figure 1 of the companion paper [6]. The initial thermal properties are shown in Table 1. The porosity and phase saturations appear in Table 2.

	C (J/kgK)	ρ (kg/m^3)	k (W/mK)
Sand (dry)	745	2,650	0.50
Water	4,200	1,000	0.50
Hydrate	2,080	917	0.46
CH_4 (test conditions)	2,518	29.5	0.034
Alluminum Alloy 2024	875	2,770	177

Table 1: Material properties

The core permeability was assumed to be 10^{-12} m^2 (consistent with the sand in the sample), although an accurate value was unimportant because practically no flow occurred during the test segments analyzed in this study. For the sand/water/gas (SWG) system, we used data from an initial thermal test (involving a step-wise increase in the bath T, following by a decrease to the original level) before the formation of hydrates. For the sand/water/gas/CH_4-hydrate (SWGH) system, we used the data corresponding to path (3) of the experiment shown in Figure 2 of the companion paper [6]. Because the conditions during these test segments provided uniformity along the z-axis, the cylindrical system (vessel and sample) could be accurately approximated by a radial system. A very fine grid (involving 445 cells of uniform Δr = 10^{-4} m) was used to describe the vessel and the core. The sample was assumed to be homogeneous and isotropic. X-ray computed tomography (CT) images [6] showed this to be a reasonable assumption during the test segments of the thermal parameter estimation study.

Calibration and Parameter Determination

Because the thermal response of a cylindrical system depends on the thermal diffusivity, it was not possible to determine simultaneously the composite specific heat C and thermal conductivity k because an infinite number of solutions (all having the same diffusivity, i.e., the C/k ratio) are possible. Thus, the specific heat of the hydrate C_H was fixed (set equal to the 2,080 J/Kg/K value reported in [1]), the composite C was computed as the sum of contributions of the sand and of the various phases, and the composite k_Θ of the sand core was then estimated through the inversion process.

The contact area between the sample and the aluminum vessel was determined to play a significant role in the calibration process. Early results indicated that the assumption of complete contact led to an unsatisfactory match between predictions and T measurements. Such an assumption was unrealistic because of the limited contact area between the sand grains and the smooth metal surface, and because of the possible occurrence of gas gaps between the vessel walls and the core. The existence of such gaps was confirmed by inspecting the high-definition CT images of the core-vessel interface (see [6]), and tended to be more pronounced after the formation of hydrate because of possible displacement in response to thermomechanical stresses. To address the problem, the interface area

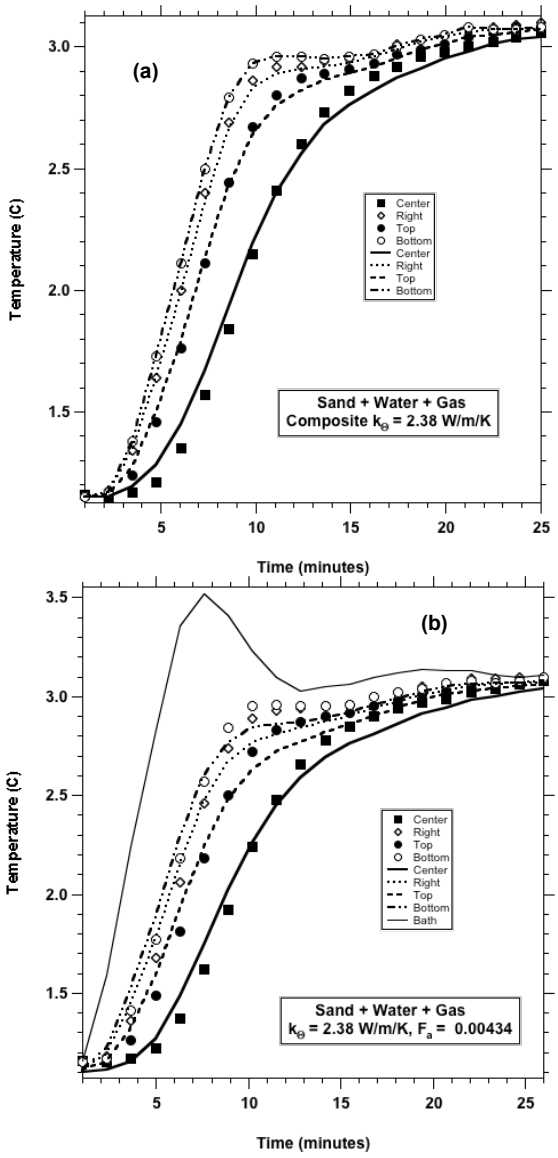

Figure 1: Calibration and parameter determination in the SWG system (symbols represent measurements, lines represent model predictions)

	SWG	SWGH
ϕ	0.38	0.38
S_W	0.52	0.19
S_H	0.00	0.36
S_G	0.48	0.45
Bulk C (kJ/kg/K)	1.116	0.940
Bulk ρ (kg/m^3)	1841	1842
k_Θ (W/m/K)	**2.380**	**3.145**
F_a	**0.00434**	**0.00217**

Table 2: Sand core saturations and properties.

(as characterized by the F_a factor, by which the vessel wall area had to be reduced) became a perturbation parameter to be determined by the inversion process in addition to k_Θ.

The iTOUGH2 [10] solutions of the inverse problem (i.e., the k_Θ and F_A values) appear in Table 2 (in boldface). Figure 1(a) shows the relationship between observations and T predictions for the optimal k_Θ = 2.380 W/m/K of the SWG system, determined from thermocouple data within the core during the stepwise increase in the bath T in the initial thermal test. Figure 1(b) shows the relationship between observations and T predictions, obtained by keeping k_Θ constant and determining the F_a value that optimizes the SWG system solution (using T data from both within the core and at the water bath boundary). Using the same k_Θ and F_a values, we conducted a forward simulation to predict T during the cooling period (step-wise reduction of the bath T) of the initial thermal test. The very good agreement between predictions and T observations in Figure 2 validates the k_Θ and F_a values. Figure 2(a) involves predictions within the core (in which only k_Θ is employed), while Figure 2(b) describes the response of the vessel-core system (and is based on both the k_Θ and the F_a values).

Figure 3 shows the relationship between observations and T predictions in the SWGH system for the optimal k_Θ and F_a values (see Table 2) determined by the inversion process. As in Figure 1, Figure 3(a) involves the determination of the optimal k_Θ from data within the core, while Figure 3(b) involves the determination of the optimal F_a for a constant k_Θ (using T data from both the boundary and the core). Note that the hydrate is stable under the conditions of this test segment. The evolution of hydrate is shown to reduce the contact area between the sample and its containing vessel, as indicated by the lower F_a value. Although liquid water and hydrate have approximately the same thermal conductivity, the significant discrepancy between the k_Θ values in the SWG and the SWGH systems casts doubts on the applicability of the linear model of Bejan [2] to hydrate-bearing systems. According to this model,

$$k_\Theta = (1-\phi)k_{Sd} + \phi S_W k_W + \phi S_H k_H \qquad (1)$$

Validity of this model would not result in the k_Θ disparity indicated by the values in Table 1. Note that because of its very low thermal conductivity, the gas contribution can be safely omitted in (1).

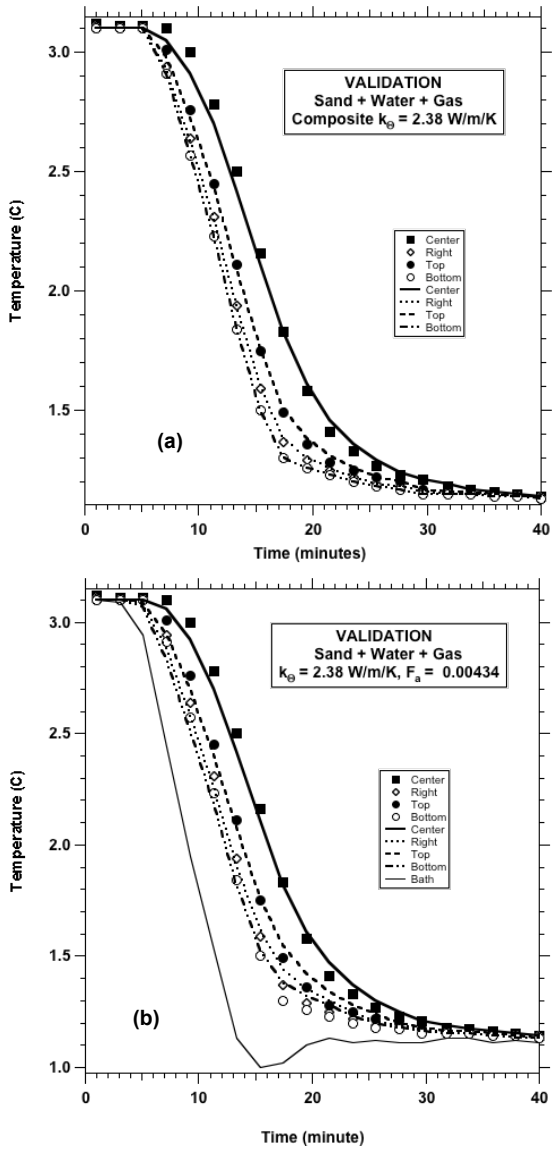

Figure 2: Prediction of cooling phase response and validation of the parameters of the SWG system (symbols represent measurements, lines represent model predictions).

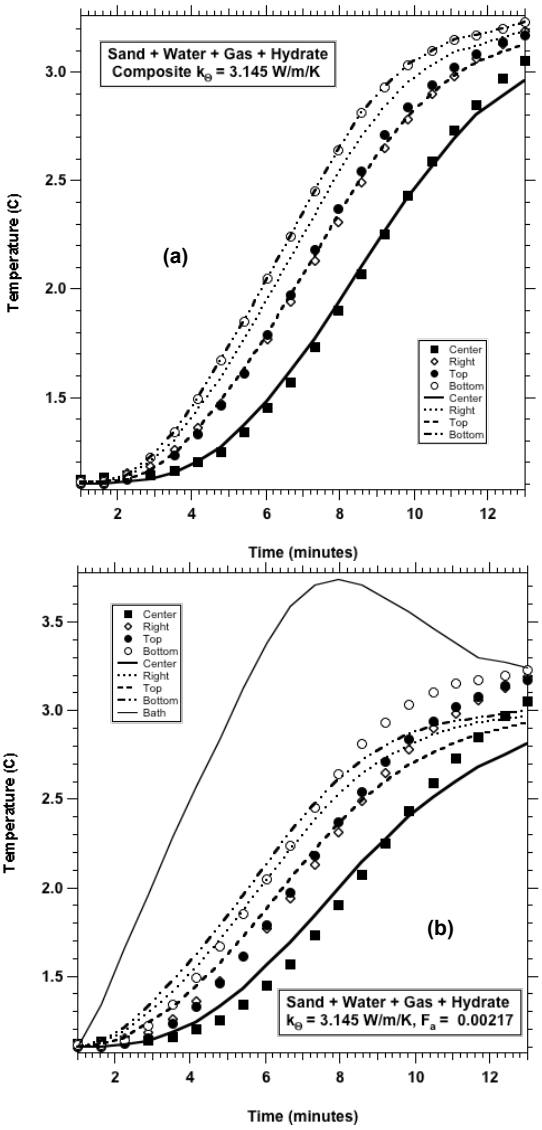

Figure 3: Calibration and parameter determination of the hydrate-bearing SWGH system (symbols represent measurements, lines represent model predictions).

A tentative thermal conductivity model

Based on the limited data provided by the thermal property analysis, we propose the following model for the estimation of thermal conductivity in hydrate bearing systems:

$$k_\Theta = (\sqrt{S_H} + \sqrt{S_W})\,(k_{Sw} - k_{Sd}) + k_{Sd} \qquad (2)$$

This is an extension of an earlier model [11,12] for k_Θ estimation in partially saturated porous media. For the sand in our experiments and the SWG system, for S_W = 0.52, S_H= 0 and k_{Sd} = 0.5 W/m/K, Equation (2) leads to an estimate of k_{Sw} = 3.1 W/m/K, which is consistent with the values reported by de Marsily [13]. For the SWGH system, when S_W = 0.19, S_H = 0.36, k_{Sd} = 0.5 W/m/K and k_{Sw} = 3.1 W/m/K, Equation (2) yields k_Θ = 3.2 W/m/K. This compares favorably with the k_Θ = 3.145 W/m/K value determined from the inversion process (Table 2).

Note that, given the very limited data on which it is based, the model described by (2) can only be described as tentative. Laboratory studies to develop the data for a more robust k_Θ model are in progress.

KINETIC PARAMETER ESTIMATION

The simulation specifics

The simulated system is depicted in Figure 1 of the companion paper [6]. The thermal and hydraulic properties in this study were the same as those dis cussed in the previous section (Tables 1 and 2).

Because determining the parameters of kinetic dissociation involved matching not only the T response of the system, but also the P behavior in the finite volume of the experiments (as well as the cumulative gas production), we could not assume linear uniformity. Therefore, the core and the containing vessel were simulated using a very fine non-uniform cylindrical grid involving 24 x 93 subdivisions in (r,z), resulting in a total of 2,232 cells and 8,928 equations. In this grid, $\Delta r = 2\text{x}10^{-3}$ m and Δz varied between $3\text{x}10^{-3}$ and $5\text{x}10^{-3}$ m. The main objective of this effort was to determine the K_0 and ΔE parameters in the kinetic model [4,5]:

$$\frac{dm_H}{dt} = K_0 \exp(\frac{\Delta E}{RT})\, A\, [f_e(T) - f] \qquad (3)$$

The term $f_e(T)$ is the fugacity at the equilibrium pressure corresponding to the temperature T. Note that the intrinsic rate of hydrate dissociation may be affected by the method of estimation of the surface area A of the dissociation reaction. From Moridis et al. [3,8], $A = A_0\,(S_H)^{2/3}$, where the 0 subscript indicates the initial value.

For the study of this SWGH system, we analyzed the data from the thermal dissociation in the two-stage heating process corresponding to the experiment paths 4 and 5 shown in Figure 2 of the companion paper [6]. The initial conditions during this thermal dissociation process are described in Table 2 (SWGH system). The assumption of uniform initial distribution of properties and saturations in

the simulations was supported by the CT images [6]. During the thermal dissociation, the temperature of the boundary (i.e., of the water bath) was raised, the system response in terms of P and T was measured, the changes in the phase saturations were quantified using CT images, and the mass of released CH_4 was determined using the CT-obtained density changes in the core -- cross-referenced against the mass computed from the evolution of P and T in the gas collection bottle (see Figure 5 in [6]).

Calibration, parameter determination, and validation

The approach followed in the calibration and parameter estimation effort followed a two-stage process that mirrored the two heating stages, and involved the simultaneous inversion of (history matching against) the P, T, and released CH_4 data using the method of Thomas and Hellums [9]. In the first stage, the optimal parameter estimates were determined by minimizing the deviation between observations from the 1st stage of thermal dissociation and predictions. The perturbation parameters were K_0, ΔE and the F_a factor. From preliminary simulations, there was sufficient evidence to indicate that F_a played a very important role in the total system response because it controlled the heat transfer between the boundary and the core. In addition to the preliminary scoping studies, the importance attached to the F_a was justified by a careful review of the CT scans, which had indicated significant displacement in the core during the thermal dissociation process (caused by thermomechanical stresses) and an increase in the contact area between the hydrate-bearing medium and the metal vessel during thermal dissociation.

Upon completing the 1st stage of the calibration process, we analyzed the data corresponding to the thermal dissociation from the 2nd heating stage. This analysis was based on the assumption K_0 and ΔE parameter validity (estimated in the 1st stage), and on the determination of the F_a factor that minimized the residuals in the optimization process. This approach was justified by the underlying hypothesis that K_0 and ΔE are intrinsic (and, consequently, invariant) parameters.

The K_0, ΔE, and F_a parameter estimates from the analysis of the two-stage thermal dissociation process are shown in Table 3. The increase in the F_a value from the 1st to the 2nd heating stage is attributed to enhanced contact between the medium and the containing metal vessel brought about by the higher P (corresponding to the higher T). Note that although constant F_a values are estimated here for each heating stage (representing time-averaged values), F_a is expected to vary in time within each stage as P and T increase.

In Figure 4, comparison of the T observations to the numerical predictions (using the optimized parameter values) at the four thermocouple locations discussed in [6] indicate an excellent agreement. For reference, the evolution of the time-variable boundary (water bath) T is included in the same figure. Figure 5 shows an excellent agreement between the observed and predicted evolution of pressure. Deviations between observations and predictions in Figures 4 and 5 do not exceed 3%.

This is not the case in Figure 6, which indicates a relatively sizeable discrepancy between observations and predictions of the amount of CH_4 released into the closed system during thermal dissociation in the 1st stage of heating. This deviation is about 11%, and is partially attributed to experimental errors and imperfections in the CH_4 mass estimation from the P and T in the gas collection bottle.

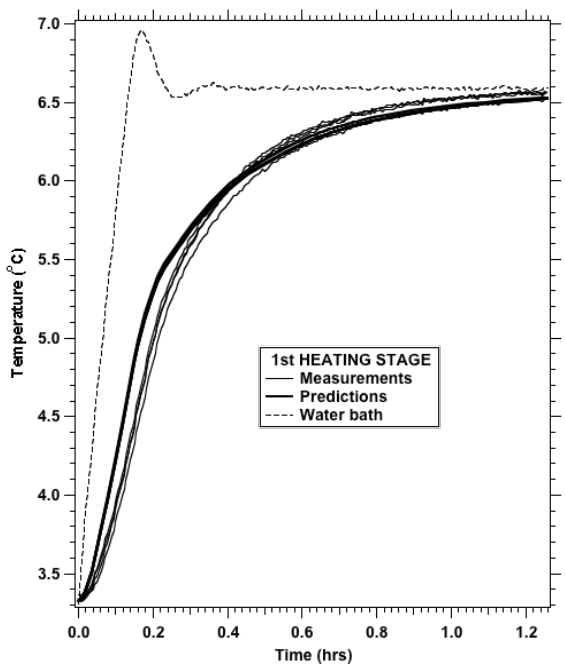

Figure 4. Observed and predicted T evolution in the core during the 1st heating stage.

Heating Stage	K_0 (mol/m^2/Pa/s)	ΔE (J/mol)	F_a
1st Stage	1.78x10^6	8.97x10^4	0.0832
2nd Stage	1.78x10^6	8.97x10^4	0.1091

Table 3: Parameter estimation for the kinetic dissociation of hydrates in a porous medium

The S_H distribution in the contour plot of Figure 7 shows that, at the end of the 1st heating stage, the hydrate in the vicinity of the metal vessel has dissociated, while S_H has increased in the center of the core. This indicates that the increased pressure and the availability of CH_4 from hydrate dissociation from the core outer surface lead to the formation of hydrate toward to core center of the core, where the max$\{S_H\}$ = 0.385 is higher than the initial value of 0.36 at the beginning of heating. These predictions are consistent with observations from x-ray CT images that show that, at the end of the 1st stage, the dissociation front had advanced by about 5 mm from the vessel wall, and that the density near the center of the core has increased slightly (indicating hydrate formation).

Figures 8, 9, and 10 show the relationship between observed and predicted *T, P* and released CH_4 mass, respectively, during the 2nd heating stage. The predictions are based on the optimized parameter values shown in Table 3. The excellent agreement between the observed and predicted data sets (differing by less than 3%) indicate the success of the two-stage history matching process and of the model calibration (from which the parameters are determined), in addition to validating (a) the parameter values determined during the history matching process, and (b) the hypothesis that K_0 and ΔE are invariant over the entire temperature range of the two stages.

Discussion

In addition to determining the parameters, the results of this study validate the hypothesis of the intrinsic character of the parameters of kinetic dissociation, and of their estimates. In addition, the excellent overall agreement between observations and numerical predictions provide additional confidence in (and support for the validation of) the TOUGH-Fx/HYDRATE model. Finally, the results indicate that predictions based on the tentative thermal conductivity model of Equation (2) (developed in the course of this study and incorporated into the TOUGH-Fx/HYDRATE code) do not pose any fundamental conflicts with the observed heat transfer behavior of the hydrate bearing system. However, the available data are insufficient to support a claim of validity of the thermal conductivity model of Equation (2). Additional laboratory studies to address the dearth of knowledge on the subject are in progress.

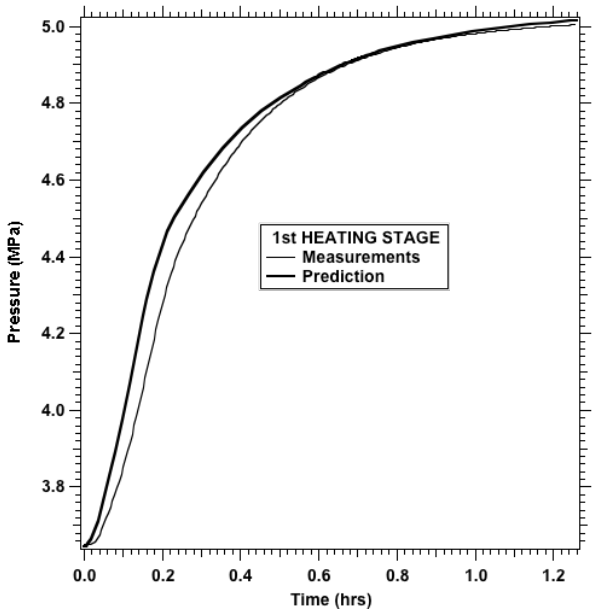

Figure 5. Observed and predicted *P* evolution in the core during the 1st heating stage.

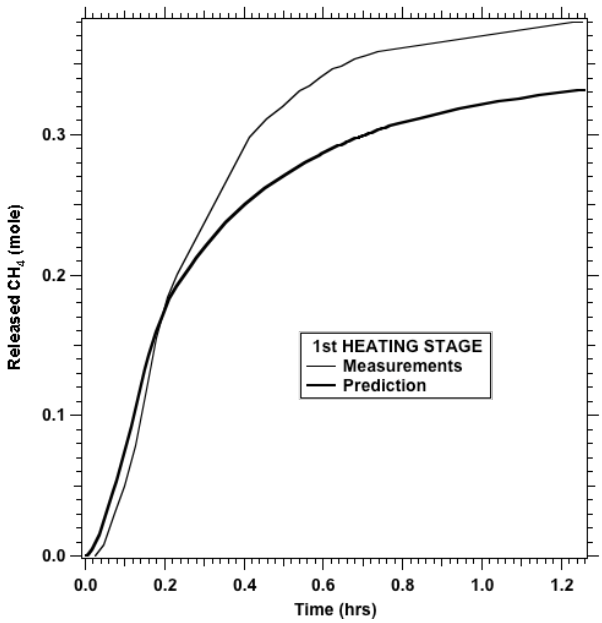

Figure 6: Observed and predicted evolution of CH_4 release during the 1st heating stage.

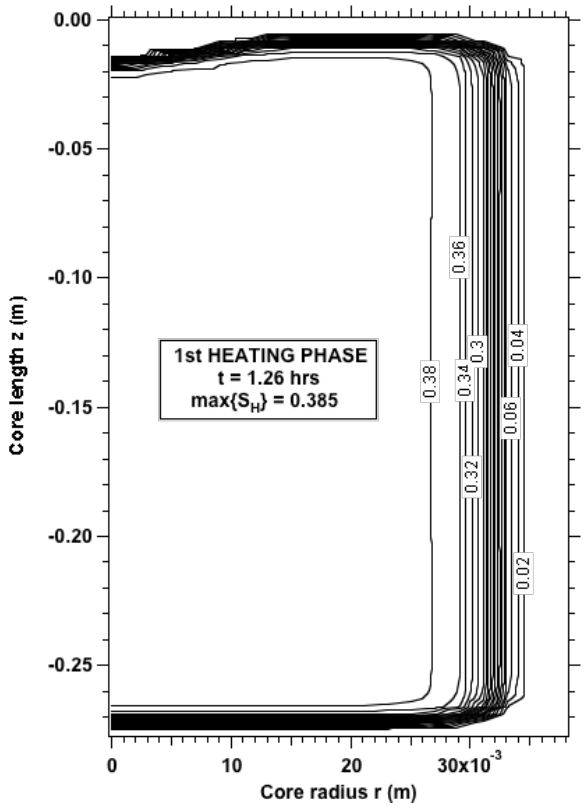

Figure 7: Hydrate saturation distribution in the core at the end of the 1st heating stage.

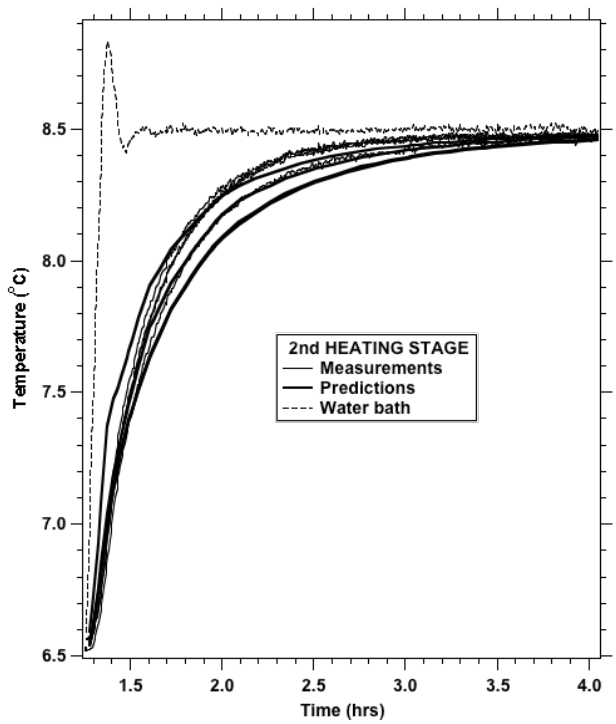

Figure 8: Observed and predicted T evolution in the core during the 2nd heating stage. The time-variable water bath T is included for reference.

The ΔE = 8.97x10^4 J/mol estimated from the inverse modeling of the laboratory data of Kneafsey et al. [6] (involving thermal dissociation of hydrates in porous media) is on the same order of magnitude, but higher than the previously reported values of Kim et al. [4] (ΔE = 7.8x10^4 J/mol) and of Clarke and Bishnoi [5] (ΔE = 8.1x10^4 J/mol). The reason for this difference is not known, but a potential explanation is the epitaxial stabilization of the hydrate by the substrate in the porous medium system.

The most striking difference between the results of this study and previously reported data is in the value of the intrinsic rate of kinetic dissociation K_0. Our estimate from this study (K_0 = 1.78x10^6 mol/m^2/Pa/s) is about 15 times larger than the Kim et al. [4] estimate (K_0 = 1.24x10^5 mol/m^2/Pa/s), and about 50 times higher than the Clarke and Bishnoi [5] (K_0 = 3.64x10^4 mol/m^2/Pa/s). It is possible that the geometric characteristics (imposed by the pore structure on the hydrate particles and the total surface area of the dissociating hydrate) are responsible for this substantial difference. Another possibility is that the value of K_0 is linked to the method of estimating the surface area A of the dissociation reaction. It is also possible that the much higher K_0 compensates for the larger ΔE determined by our study. Because of the very significant computation time requirements, the subject has not been thoroughly investigated, and the sensitivity of the hydrate dissociation rate to the K_0 and ΔE parameters has not yet been completed. Additional numerical studies (currently in progress) are expected to address the issue.

SUMMARY AND CONCLUSIONS

This study is based on the analysis of the laboratory data from the investigation of Kneafsey et al. [6]. These data were obtained during the process of controlled hydrate formation and dissociation in porous media, and involve pressure and temperature measurements in addition to CT images.

To limit uncertainty and the possibility of non-uniqueness in the solutions of the inverse problem, the study proceeded in two phases. The first phase focused exclusively on determining the thermal properties, while the second phase concentrated on estimating the kinetic parameters of the reaction.

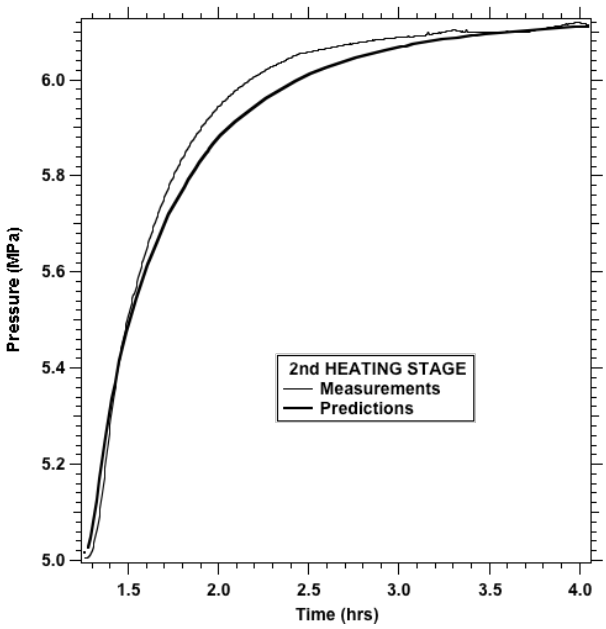

Figure 9: Observed and predicted P evolution in the core during the 2nd heating stage.

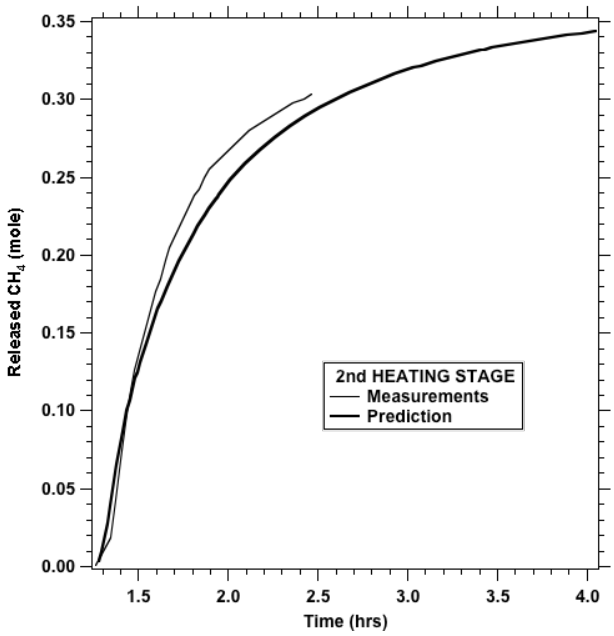

Figure 10: Observed and predicted mass of released CH_4 during the 2nd heating stage.

By numerically inverting (history matching) the thermal response of the system (a) before the formation of the hydrate and (b) within the hydrate stability zone (i.e., before the onset of hydrate dissociation), we determined the thermal properties of the composite system (composed of the porous medium and the various pore-occupying fluid and solid phases). Additionally, we developed a tentative model describing the dependence of the composite thermal conductivity of hydrate-bearing media on the phase distribution in the pores.

Using the thermal properties from the first phase of the study, we determined the parameters describing the system response by means of inverse modeling of data from a two-stage heating (and thermal dissociation) of the hydrate-bearing core, and by combining P and T measurements with x-ray CT image analysis. In addition to the kinetic parameters, the contact area between the core and the containing vessel (a very important factor in heat transfer) was determined from the 1st heating stage. The kinetic parameters from the 1st heating stage were used for history matching the results of the 2nd heating stage, from which the vessel-core contact area was estimated for this specific stage. The excellent agreement between observations and numerical predictions validated the parameters determined through the inversion process, confirmed the hypothesis of their intrinsic character (and, thus, invariant values), provided increased confidence in (and further verification of) the numerical model used to describe the hydrate behavior in porous media, and indicated that the thermal conductivity model was not inconsistent with the overall system behavior.

Compared to previously published values, our estimates of the kinetic parameters indicated a higher activation energy (ΔE = 8.97x10^4 J/mol), but on the same order of magnitude with earlier literature estimates. Conversely, the intrinsic energy of dissociation (K_0 = 1.78x10^6 mol/m^2/Pa/s) is between one and two orders of magnitude larger than previously reported values. The reason for this discrepancy is not well known because the effect of the porous medium on the hydrate dissociation process is not yet fully understood. Additional studies to address the issue are in progress.

ACKNOWLEDGEMENT

This work was supported by the Assistant Secretary for Fossil Energy, Office of Natural Gas and Petroleum Technology, through the National Energy Technology Laboratory, under U.S. DOE Contract No. DE-AC03-76SF00098. The authors thank John Apps, Stefan Finsterle and Dan Hawkes for their helpful review comments.

REFERENCES

[1] Sloan, E.D., Clathrate Hydrates of Natural Gases. 1998, New York: Marcel Dekker. 705.

[2] Bejan, A., Convection Heat Transfer. 1984, New York: John Wiley & Sons. 416.

[3] Moridis, G.J., et al., Analysis and interpretation of the thermal test of gas hydrate dissociation in the Mallik 5L-38 Research Well, Mackenzie Delta, Canada, in *Scientific Results from the Mallik 2002 Gas Hydrate Production Research Well Program, Mackenzie Delta, Northwest Territories, Canada*. 2005. Geological Survey of Canada, Bulletin 585.

[4] Kim, H.C., et al., Kinetics of Methane Hydrate Decomposition. *Chem. Eng. Sci.*, 1987. **42, No. 7**: p. 1645-1653.

[5] Clarke, M. and P.R. Bishnoi, Determination of the Activation Energy and Intrinsic Rate Constant of Methane Hydrate Decomposition. *Canadian Journal of Chemical Engineering*, 2001. **79**(1): p. 143-147.

[6] Kneafsey, T., et al., Methane hydrate formation and dissociation in partially saturated sand -- Measurements and Observations, in *Fifth International Conference on Gas Hydrates*. 2005. Trondheim, Norway.

[7] Moridis, G.J., Numerical Studies of Gas Production From Methane Hydrates. *SPE Journal*, 2003. **32**(8): p. 359-370.

[8] Moridis, G.J., et al., TOUGH-Fx /HYDRATE: A code for the simulation of system behavior in hydrate-bearing geologic media. 2005. Lawrence Berkeley National Laboratory (Report No. pending).

[9] Thomas, L.K., and L.J. Hellums, A Nonlinear Automatic History Matching Technique for Reservoir Simulation Models (SPE 3475, 1972), in *SPE Reprint Series*, No.11, 1973. SPE, p. 106-112.

[10] Finsterle, S., iTOUGH2 User's Guide, 1997. Lawrence Berkeley National Laboratory Report LBNL-40400.

[11] Somerton, W.H., et al., Thermal behavior of unconsolidated oil sands. 1973. Paper SPE-4506, 48th Annual Fall Meeting of the Society of Petroleum Engineers, Las Vegas, NV.

[12] Somerton, W.H., et al., High temperature behavior of rocks associated with geothermal type reservoirs. 1974. Paper SPE-4897, 44th Annual California Regional Meeting of the Society of Petroleum Engineers, San Francisco, CA.

[13] de Marsily, G., Quantitative Hydrogeology. 1986, San Diego: Academic Press. 440.